Dynamics of k-core percolation in a random graph

Mami Iwata and Shin-ichi Sasa §

Department of Pure and Applied Sciences, University of Tokyo, Komaba, Tokyo
153-8902, Japan

Abstract. We study the edge deletion process of random graphs near a k-core
percolation point. We find that the time-dependent number of edges in the process
exhibits critically divergent fluctuations. We first show theoretically that the k-core
percolation point is exactly given as the saddle-node bifurcation point in a dynamical
system. We then determine all the exponents for the divergence based on a universal
description of fluctuations near the saddle-node bifurcation.

1. Introduction

We study the following time evolution of random graphs on n vertices. Let us denote one
sample trajectory of graphs by $\{G(t)\}_{0 \le t \le \infty}$, where the time t is a real number. $G(0)$ is
assumed to contain m edges that connect two vertices chosen randomly. Here, $R = m/n$
is regarded as a control parameter of the model. When $t > 0$, a vertex is chosen with a
constant rate α for each vertex. Then, if the number is less than an integer k, all the
edges incident to the vertex are deleted. This rule defines the Poisson jump process $G(t)$
in the set of graphs on n vertices. We display two examples of the time evolution of
graphs in Fig. 1, where the random graphs are embedded in the two-dimensional space.

Let $\mu(t)$ be the number of edges at time t. Obviously, when R is sufficiently small,
$\mu(t = \infty)/n$ is zero with probability 1 in the limit $n \to \infty$. It has been known that
there is a critical value of R above which $\mu(\infty)/n$ is finite (nonzero) with probability 1
in the same limit [1]. The final graph provides the k-core (See Fig. 1), which is defined
by the largest subgraph with minimum degree at least k. This transition with respect
to the change in R is called the k-core percolation in a random graph. The critical value
$R_{\rm c}$ was calculated exactly in Ref. [1].

The k-core percolation was studied in several research fields such as magnetism [2],
rigidity percolation [3], jamming transitions [4, 5], and network problems [6, 7]. It is
also related to the random field Ising model, which is a representative model exhibiting
so-called avalanches [8, 9]. In particular, the dynamics of k-core percolation might be
considered from the viewpoint of the vulnerability of a network to random node attack
[10].

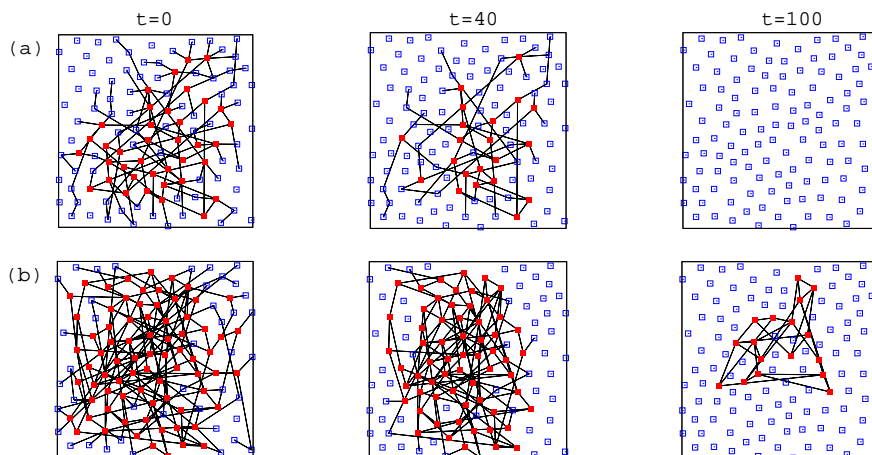§ To whom correspondence should be addressed (sasa@jiro.c.u-tokyo.ac.jp).

Figure 1. Time evolution of random graphs from initial states (left) to final states (right). $k = 3$, $n = 118$, and $R = 1.0$ (a) and $R = 1.7$ (b), respectively. The final state in the case $R = 1.7$ corresponds to the 3-core. The filled square symbol (red online) at each time represents a heavy vertex and open square symbol (blue online) a light vertex.

In this paper, we wish to elucidate the nature of the dynamics near the transition point. Concretely, let h be the number of vertices with degree at least k. (Such a vertex is called a *heavy vertex*; otherwise, a *light vertex*.) We are interested in the time evolution of h. As an example, we present the results of numerical simulations in Fig. 2. ‖ Here, the ensemble average $\langle h(t)/n \rangle$ and its fluctuation intensity $\chi(t) \equiv \langle (h(t) - \langle h(t) \rangle)^2/n \rangle$ are displayed as functions of t. Figure 2 indicates that $\chi(t)$ has one peak at $t = \tau$, and we conjecture that τ and $\chi(\tau)$ exhibit the power-law divergences $\tau \simeq \epsilon^{-\zeta}$ and $\chi(\tau) \simeq \epsilon^{-\gamma}$, where $\epsilon = R_c - R > 0$. Indeed, we will derive these divergences theoretically and determine the values $\zeta = 1/2$ and $\gamma = 5/2$.

The divergent behavior observed near the percolation point suggests the existence of critical fluctuations. On the other hand, it has been known that a giant k-core appears in the discontinuous manner at the transition point for cases $k \geq 3$. Such coexistence of the discontinuous transition and critical fluctuations has been emphasized in relation to the nature of jamming and glass transitions [11, 12, 13]. Therefore, the theoretical description of the divergent behavior near the k-core percolation may provide a new insight toward understanding of jamming and glassy systems.

This paper is organized as follows. In Sec. 2, we present a master equation for four variables that characterize a graph. Since this master equation was derived rigorously in Ref. [1], our presentation in this paper is based on an intuitive argument understandable for physicists. Then, in Sec. 3, by considering the situation with large n, we derive a Langevin equation for the four variables. The Langevin equation is analyzed in the subsequent two sections. In Sec. 4, we find a saddle-node bifurcation for the rate

‖ In numerical simulations, we generate a chain of waiting time obeying the Poisson distribution and choose a vertex randomly with these time intervals.
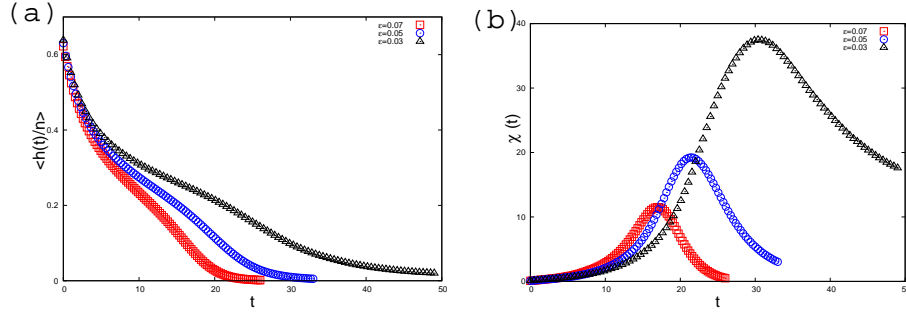
Figure 2. Relaxation behavior of heavy vertex density $\langle h(t)/n \rangle$ (a) and its fluctuation intensity $\chi(t)$ (b). $\epsilon = 0.03$, $\epsilon = 0.05$, and $\epsilon = 0.07$. $k = 3$, $\alpha = 1$, and $n = 4096$.

equation obtained by the limit $n \to \infty$. Here, the bifurcation point corresponds to the k-core percolation point. Then, in Sec. 5, we study effects of noise near the bifurcation point and calculate the exponents that characterize critical divergences. The final section is devoted to concluding remarks. In order to simplify the argument, we consider the case $k = 3$. The generalization to cases $k \geq 3$ is straightforward, and essentially the same results are obtained.

2. Master equation

Let Δt be a sufficiently small time interval. We can describe the stochastic process by the transition probability $P(G'|G)$, which is the probability that $G(t + \Delta t) = G'$ under the condition that $G(t) = G$. Since $P(G'|G)$ is a huge matrix, we cannot treat it directly. Hence, we wish to have a simple description of the dynamics. The simplification of the dynamics of $G(t)$ consists of two steps. In the first step, we describe the dynamics in terms of the characteristic quantities of the graph such as the number of edges μ and the number of vertices v_r with degree r, where $r = 0, 1, \cdots$. Among them, the number of light vertices, v_0, v_1 and v_2 are directly related to the dynamics of the graph because all the edges incident to a chosen light vertex will be deleted in the next change of the graph. Indeed, according to Ref. [1], ¶ the time evolution of the four-tuple $\boldsymbol{w} = (\mu, v_0, v_1, v_2)$ is described by a Markov process. Mathematically, the probability of $\boldsymbol{w}'$ at time $t + \Delta t$ provided that $\boldsymbol{w}$ at time t is given, which is denoted by $p(\boldsymbol{w}'|\boldsymbol{w})$, is expressed as a function of $\boldsymbol{w}'$ and $\boldsymbol{w}$ for general n. (See proposition 1 in Ref. [1].) Subsequently, in the second step of the simplification, the asymptotic formula of $p(\boldsymbol{w}'|\boldsymbol{w})$ for large n is derived. (See Corollary 1 in Ref. [1].)

In this paper, we do not review the derivation of the asymptotic form $p(\boldsymbol{w}'|\boldsymbol{w})$ in Ref. [1]. Instead, we provide its mathematically naive derivation by focusing on cases

¶ Note that the edge deletion process in Ref. [1] is not identical to the dynamics we define. First, their dynamics are given as a discrete process. Second, in their dynamics, a non-isolated light vertex is always chosen at each time step. Thus, as time goes on, the deletion in their dynamics is accelerated more than that in our evolution rule. Despite this difference, one can transform mathematical statements in [1] to those valid in our model.

with large n from the outset. More precisely, we estimate $p(\boldsymbol{w}'|\boldsymbol{w})$ assuming that v_r/n with $r \geq 3$ takes the most probable value hq_r/n, where from the law of large numbers, q_r is equal to the probability that r edges are incident to a given heavy vertex under the condition that $\boldsymbol{w}$ is specified. (Recall that h represents the number of heavy vertices that is equal to $\sum_{r \geq k=3} v_r$.) We express this statement formally as

$$\frac{v_r}{h} = q_r, \tag{1}$$

where the probability q_r is given by the Poisson distribution

$$q_r = \frac{1}{r!} \frac{1}{Q(z)} z^r e^{-z} \tag{2}$$

with the normalization constant

$$Q(z) = e^{-z}(e^z - 1 - z - z^2/2). \tag{3}$$

Although the appearance of the Poisson distribution seems natural, its mathematical proof is not simple. (See Ref. [1].) Here, using the trivial relation[+] $2\mu - v_1 - 2v_2 = \sum_{r=3}^{\infty} rv_r$, we have

$$\frac{2\mu - v_1 - 2v_2}{h} = \sum_{r=3}^{\infty} rq_r, \tag{4}$$

which determines z in (2) and (3) for a given $\boldsymbol{w}$. Since the direct calculation using (2) leads to

$$\sum_{r=3}^{\infty} rq_r = \frac{z\Pi(z)}{Q(z)} \tag{5}$$

with

$$\Pi(z) = e^{-z}(e^z - 1 - z), \tag{6}$$

we obtain a useful relation for the determination of z from $\boldsymbol{w}$:

$$\frac{2\mu - v_1 - 2v_2}{h} = \frac{z\Pi(z)}{Q(z)}. \tag{7}$$

In the argument below, z always represents the unique solution of (7) for a given $\boldsymbol{w}$. Furthermore, one can easily confirm the relation

$$z = \sum_{r \geq 4} rq_r, \tag{8}$$

which provides us a simple interpretation of z.

Now, we estimate $p(\boldsymbol{w}'|\boldsymbol{w})$. We first notice the value of $\mu' - \mu$. (Note that $\mu' - \mu$ represents the change of the number of edges during the time interval Δt.) (i) When $\mu' - \mu = 0$, no deletion occurs. This implies $\boldsymbol{w}' = \boldsymbol{w}$. (ii) When $\mu' - \mu = -1$, one edge incident to a chosen vertex is deleted. This edge connects the chosen vertex with

---

[+] We express an edge by a pair of integers (ℓ_1, ℓ_2) when the edge links a vertex of degree ℓ_1 and another vertex of degree ℓ_2. Collecting all the pairs of integers for the μ edges, we have 2μ integers. Here, count the number of integers that are greater than 2.

j	$\boldsymbol{\sigma}$	$r(\boldsymbol{\sigma}|\boldsymbol{w})$
1	(-1,2,-2,0)	$\alpha v_1 p_1/n$
2	(-1,1,0,-1)	$\alpha v_1 p_2/n$
3	(-1,2,-1,1)	$\alpha v_1 p_3/n$
4	(-1,1,-1,0)	$\alpha v_1 p_4/n$

Table 1. Rate $r(\boldsymbol{\sigma}_j|\boldsymbol{w})$ for the transition $\boldsymbol{w} \to \boldsymbol{w} + \boldsymbol{\sigma}_j$. $p_j = jv_j/(2\mu)$ for $1 \le j \le 3$, and $p_4 = zh/(2\mu)$.

another vertex with degree ℓ. Then, $\boldsymbol{w}' - \boldsymbol{w}$ takes four values depending on $\ell = 1, 2, 3$, and $\ell \ge 4$, which are denoted by $\boldsymbol{\sigma}_j$ with $j = 1, 2, 3$ and $\boldsymbol{\sigma}_4$, respectively. (See Table. 1.) (iii) When $\mu' - \mu = -2$, two edges incident to a chosen vertex are deleted. Each edge connects the chosen vertex to another vertex with degree ℓ_i, $i = 1, 2$, where $\ell_i = 1, 2, 3$ or $\ell_i \ge 4$. We assume $\ell_1 \le \ell_2$ without loss of generality. Then, $\boldsymbol{w}' - \boldsymbol{w}$ takes ten values depending on the values of ℓ_1 and ℓ_2, which are denoted by $\boldsymbol{\sigma}_j$, $5 \le j \le 14$, where the correspondence between j and (ℓ_1, ℓ_2) is shown in Table 2. (iv) We do not need to consider the cases $\mu' - \mu \le -3$. Although such cases appear when deletions occur twice or more during the time interval, the probability of their occurrence is negligible for sufficiently small Δt. To sum up, $\boldsymbol{w}' - \boldsymbol{w}$ takes either $\boldsymbol{0}$ or $\boldsymbol{\sigma}_j$, $j = 1, \cdots, 14$, and the fourteen transitions occur independently.

We denote the rate of transition $\boldsymbol{w} \to \boldsymbol{w} + \boldsymbol{\sigma}$ by $r(\boldsymbol{\sigma}|\boldsymbol{w})$. We can then write

$$p(\boldsymbol{w}'|\boldsymbol{w}) = n\Delta t \sum_{j=1}^{14} r(\boldsymbol{\sigma}_j|\boldsymbol{w})\delta(\boldsymbol{\sigma}_j, \boldsymbol{w}' - \boldsymbol{w}) \tag{9}$$

when $\boldsymbol{w}' \ne \boldsymbol{w}$. $\delta(\boldsymbol{x}, \boldsymbol{y})$ is the four-dimensional Kronecker delta function for $\boldsymbol{x}$, $\boldsymbol{y}$ in $\mathbf{N}^4$. $p(\boldsymbol{w}|\boldsymbol{w})$ is determined from the normalization condition of the probability.

Let us estimate the transition rate $r(\boldsymbol{\sigma}_j|\boldsymbol{w})$. Recall that a vertex is randomly chosen at the rate α (per unit time and per each vertex). Then, the probability that the degree of the chosen vertex equals to one is given by v_1/n. We next consider the conditional probability that the edge incident to the chosen vertex connects it with a vertex of degree r. This probability, which is denoted by c_r, takes a complicated form for general cases. (See Ref. [1]). Here, notice that $rv_r/2\mu$ is the probability of finding a vertex with degree r when we observe one vertex connected to an edge, which we choose randomly. The difference between c_r and $rv_r/2\mu$ originates from the condition under which an edge is chosen. The difference is negligible for sufficiency large n. Combining these results, the rate $r(\boldsymbol{\sigma}_j|\boldsymbol{w})$ is estimated as

$$r(\boldsymbol{\sigma}_j|\boldsymbol{w}) = \alpha\frac{v_1}{n}\frac{jv_j}{2\mu} \tag{10}$$

for $1 \le j \le 3$, and

$$r(\boldsymbol{\sigma}_4|\boldsymbol{w}) = \alpha\frac{v_1}{n}\sum_{r=4}^{\infty}\frac{rv_r}{2\mu}. \tag{11}$$

j	(ℓ_1, ℓ_2)	$\boldsymbol{\sigma}$	$r(\boldsymbol{\sigma}|\boldsymbol{w})$
5	(1,1)	(-2,3,-2,-1)	$\alpha v_2 p_1^2/n$
6	(1,2)	(-2,2,0,-2)	$2\alpha v_2 p_1 p_2/n$
7	(1,3)	(-2,2,-1,0)	$2\alpha v_2 p_1 p_3/n$
8	$(1, \geq 4)$	(-2,2,-1,-1)	$2\alpha v_2 p_1 p_4/n$
9	(2,2)	(-2,1,2,-3)	$\alpha v_2 p_2^2/n$
10	(2,3)	(-2,1,1,-1)	$2\alpha v_2 p_2 p_3/n$
11	$(2, \geq 4)$	(-2,1,1,-2)	$2\alpha v_2 p_2 p_4/n$
12	(3,3)	(-2,1,0,1)	$\alpha v_2 p_3^2/n$
13	$(3, \geq 4)$	(-2,1,0,0)	$2\alpha v_2 p_3 p_4/n$
14	$(\geq 4, \geq 4)$	(-2,1,0,-1)	$\alpha v_2 p_4^2/n$

Table 2. Rate $r(\boldsymbol{\sigma}_j|\boldsymbol{w})$ for the transition $\boldsymbol{w} \to \boldsymbol{w} + \boldsymbol{\sigma}_j$. $p_j = jv_j/(2\mu)$ for $1 \leq j \leq 3$, and $p_4 = zh/(2\mu)$.

Here, it should be noted that v_3 and $\sum_{r=4}^{\infty} rv_r$ in (10) and (11) are calculated from (1) with z determined by (7). For convenience of later calculation, we summarize the result in Table 1. In this table, we introduce $p_j = jv_j/(2\mu)$ for $1 \leq j \leq 3$, and $p_4 = \sum_{r=4}^{\infty} rv_r/(2\mu) = zh/(2\mu)$. (We used (8) in deriving the latter equality.) The transition rate $r(\boldsymbol{\sigma}_j|\boldsymbol{w})$ with $5 \leq j \leq 14$ is calculated in the same manner by noting that two edges incident to one vertex can be treated independently. The result is summarized in Table 2. In the argument below, we set $\alpha = 1$ for simplicity.

Before closing this section, we consider the initial condition $\boldsymbol{w}(0)$. In order to simplify the argument, we assume that $\boldsymbol{w}(0)/n$ takes the most probable value in the limit $n \to \infty$. Let us calculate this value. We first consider the probability that k edges are incident to a vertex chosen randomly:

$$P_k = \frac{{}_{(n-1)}C_k \cdot {}_{(N-n+1)}C_{(m-k)}}{{}_N C_m}, \tag{12}$$

where $N = {}_n C_2$. Taking the limit $n \to \infty$ with fixing $R(= m/n)$, we obtain

$$P_k = \frac{1}{k!}(2R)^k e^{-2R}. \tag{13}$$

This leads to

$$\boldsymbol{w}(0) = (m, ne^{-2R}, n(2R)e^{-2R}, n(2R)^2 e^{-2R}/2). \tag{14}$$

3. Langevin equation

We define the density variable $\boldsymbol{\rho} = (\bar{\mu}, \rho_0, \rho_1, \rho_2)$ by $\boldsymbol{w}/n$. When n is large, the dynamics of $\boldsymbol{\rho}$ are expected to be described by a Langevin equation. We shall derive the equation from the transition probability $p(\boldsymbol{w}'|\boldsymbol{w})$ given in (9) with Tables 1 and 2.

We utilize an expansion formula of the Kronecker delta function

$$\delta(x, y) = \int_{-\pi}^{\pi} \frac{du}{2\pi} e^{iu(x-y)} \tag{15}$$

for any x and y in $\mathbf{N}$. Substituting this formula into (9), we obtain

$$p(n\boldsymbol{\rho}'|n\boldsymbol{\rho}) = n\Delta t \int_{\mathcal{D}} \frac{d^4\boldsymbol{u}}{(2\pi n)^4} e^{-i\boldsymbol{u}\cdot(\boldsymbol{\rho}'-\boldsymbol{\rho})} \sum_{j=1}^{14} r(\boldsymbol{\sigma}_j|n\boldsymbol{\rho}) e^{i\boldsymbol{u}\cdot\boldsymbol{\sigma}_j/n} \tag{16}$$

for $\boldsymbol{\rho}' \neq \boldsymbol{\rho}$, where $\mathcal{D} = [-n\pi, n\pi]^4$. Noting $p(n\boldsymbol{\rho}|n\boldsymbol{\rho}) = 1 - \sum_{j=1}^{14} r(\boldsymbol{\sigma}_j|\boldsymbol{w})n\Delta t$, we can write

$$p(n\boldsymbol{\rho}'|n\boldsymbol{\rho}) = \int_{\mathcal{D}} \frac{d^4\boldsymbol{u}}{(2\pi n)^4} e^{-i\boldsymbol{u}\cdot(\boldsymbol{\rho}'-\boldsymbol{\rho})} \mathcal{F}(\boldsymbol{\rho}) \tag{17}$$

for any $\boldsymbol{\rho}'$ and $\boldsymbol{\rho}$, where $\mathcal{F}$ is expressed as

$$\mathcal{F}(\boldsymbol{\rho}) = n\Delta t \sum_{j=1}^{14} r(\boldsymbol{\sigma}_j|n\boldsymbol{\rho}) e^{i\boldsymbol{u}\cdot\boldsymbol{\sigma}_j/n} + \left(1 - \sum_{j=1}^{14} r(\boldsymbol{\sigma}_j|n\boldsymbol{\rho})n\Delta t\right)$$

$$= \exp\left(\sum_{j=1}^{14} r(\boldsymbol{\sigma}_j|n\boldsymbol{\rho})n\Delta t \left(e^{i\boldsymbol{u}\cdot\boldsymbol{\sigma}_j/n} - 1\right) + O(\Delta t^2)\right)$$

$$\simeq \exp\left(\sum_{j=1}^{14} r(\boldsymbol{\sigma}_j|n\boldsymbol{\rho})n\Delta t \left(i\boldsymbol{u}\cdot\boldsymbol{\sigma}_j/n - (\boldsymbol{u}\cdot\boldsymbol{\sigma}_j)^2/(2n^2)\right)\right), \tag{18}$$

where we have ignored the terms of $O((\Delta t)^2, \Delta t/n^2)$. Here, we first consider the case with large n and then assume Δt to be sufficiently small. We then have the transition probability

$$p(n\boldsymbol{\rho}'|n\boldsymbol{\rho}) = \int_{\mathbf{R}^4} \frac{d^4\boldsymbol{u}}{(2\pi n)^4} \exp\left[-i\boldsymbol{u}\cdot\left(\boldsymbol{\rho}' - \boldsymbol{\rho} - \sum_{j=1}^{14} r(\boldsymbol{\sigma}_j|n\boldsymbol{\rho})\Delta t\boldsymbol{\sigma}_j\right)\right.$$

$$\left. - \sum_{j=1}^{14} r(\boldsymbol{\sigma}_j|n\rho)\Delta t (\boldsymbol{u}\cdot\boldsymbol{\sigma}_j)^2 \frac{1}{2n}\right]. \tag{19}$$

Here, we define a 4×4 matrix

$$A_{lm}(n\boldsymbol{\rho}) \equiv \sum_{j=1}^{14} \frac{r(\boldsymbol{\sigma}_j|n\boldsymbol{\rho})}{2}(\boldsymbol{\sigma}_j)_l(\boldsymbol{\sigma}_j)_m. \tag{20}$$

Since the matrix $\hat{A} = (A_{lm})$ is semi-positive, there exists the semi-positive matrix $\hat{G}$ satisfying $\hat{A} = \hat{G}^2$. We also define $\Delta\boldsymbol{\Xi}$ by

$$\hat{G}(n\boldsymbol{\rho})\Delta\boldsymbol{\Xi} \equiv \boldsymbol{\rho}' - \boldsymbol{\rho} - \sum_{j=1}^{14} r(\boldsymbol{\sigma}_j|n\boldsymbol{\rho})\Delta t\boldsymbol{\sigma}_j. \tag{21}$$

Then, the probability density of $\Delta\boldsymbol{\Xi}$ is expressed as

$$p(\Delta\boldsymbol{\Xi}) = \det(\hat{G})n^4 p(n\boldsymbol{\rho}'|n\boldsymbol{\rho}), \tag{22}$$

where $\det(\hat{G})$ is the determinant of the Jacobian matrix associated with the transformation from $\boldsymbol{\rho}'$ to $\Delta\boldsymbol{\Xi}$, and note that the probability density of $\boldsymbol{\rho}'$ is given by $n^4 p(n\boldsymbol{\rho}'|n\boldsymbol{\rho})$, because $\int d^4\boldsymbol{\rho}' p(n\boldsymbol{\rho}'|n\boldsymbol{\rho}) = \sum_{\boldsymbol{w}'} p(\boldsymbol{w}'|n\boldsymbol{\rho})/n^4 = 1/n^4$. From (19) and (22), we obtain

$$p(\Delta\boldsymbol{\Xi}) = \frac{n^2}{16\pi^2(\Delta t)^2} e^{-\frac{n}{4\Delta t}(\Delta\boldsymbol{\Xi})(\Delta\boldsymbol{\Xi})}. \tag{23}$$

This implies that $\Delta\boldsymbol{\Xi}$ is the Gaussian noise satisfying

$$\langle \Delta\Xi_l \Delta\Xi_m \rangle \equiv \frac{2\Delta t}{n} \delta_{lm}. \tag{24}$$

Taking the limit $\Delta t \to 0$ in (21) with (24), we obtain

$$\partial_t \boldsymbol{\rho} = \sum_{j=1}^{14} r(\boldsymbol{\sigma}_j | n\boldsymbol{\rho})\boldsymbol{\sigma}_j + \sqrt{\frac{1}{n}}\hat{G}(n\boldsymbol{\rho}) \cdot \boldsymbol{\xi}, \tag{25}$$

with $\langle \xi_l(t)\xi_m(t') \rangle = 2\delta(t-t')\delta_{lm}$. Here, the symbol $''\cdot''$ in (25) represents the Ito rule of the multiplication of stochastic variables. Finally, from (14), the initial condition of the Langevin equation is given by

$$\boldsymbol{\rho}(0) = (R, e^{-2R}, (2R)e^{-2R}, (2R)^2 e^{-2R}/2). \tag{26}$$

4. Deterministic equation

The Langevin equation (25) becomes the deterministic equation in the limit $n \to \infty$:

$$\partial_t \boldsymbol{\rho} = \sum_{j=1}^{14} r(\boldsymbol{\sigma}_j | n\boldsymbol{\rho})\boldsymbol{\sigma}_j. \tag{27}$$

Concretely, using Tables 1 and 2, we can obtain the expression

$$\partial_t \bar{\mu} = -s, \tag{28}$$

$$\partial_t \rho_0 = \rho_1 + \rho_2 + \rho_1 \frac{s}{2\bar{\mu}}, \tag{29}$$

$$\partial_t \rho_1 = -\rho_1 - \rho_1 \frac{s}{2\bar{\mu}} + 2\rho_2 \frac{s}{2\bar{\mu}}, \tag{30}$$

$$\partial_t \rho_2 = -\rho_2 - 2\rho_2 \frac{s}{2\bar{\mu}} + 3\rho_3 \frac{s}{2\bar{\mu}}, \tag{31}$$

where $s = \rho_1 + 2\rho_2$ is the density of the edges incident to light vertices, and $\rho_3 = v_3/n$ is determined as a function of $\boldsymbol{\rho}$ from (1) with z determined by (7). The derivation of (28)-(31) requires tedious calculation, while the result is understood intuitively. For example, the third term of (29) represents the change in the degree of a vertex from 1 to 0 by the deletion of the edge connecting this vertex with another vertex that is chosen randomly. The differential equation given in (28) - (31) with the initial condition (26) determines the most probable behavior of the Langevin equation (25).

Putting aside the initial condition, we study the differential equation in (28) - (31). The complicated nature arises from the implicit dependence of ρ_3 on $\boldsymbol{\rho}$ through z. In order to avoid it, we carry out the transformation of variables. First, we choose z as a dynamical variable. Taking the derivative of (7) with respect to time, we obtain

$$\partial_t z = -\frac{sz}{2\bar{\mu}}. \tag{32}$$

Seeing (28) and (32), we further choose s as a dynamical variable. We then obtain

$$\partial_t s = -s - \frac{s^2}{2\bar{\mu}} + 3\frac{v_3 s}{\bar{\mu}}. \tag{33}$$

Thus, (28), (30), (32), and (33) constitute the differential equation for $(\bar{\mu}, \rho_1, s, z)$, which is equivalent to the differential equation for $\boldsymbol{\rho}$. Here, from (28) and (32), we find immediately a constant of motion

$$J_1 = \frac{z^2}{\bar{\mu}}. \tag{34}$$

Furthermore, noting $\partial_t \bar{h} = -3\rho_3 s/(2\bar{\mu})$ and $\partial_z Q = z^2 e^{-z}/2$, one confirms that there is another constant of motion

$$J_2 = \frac{\bar{h}}{Q(z)}, \tag{35}$$

where $\bar{h} = h/n$. Recalling (7), we rewrite J_2 as $J_2 = z\Pi(z)/(2\bar{\mu} - s)$. Now, defining $J_3 = J_1 J_2/2$, we obtain the expression

$$s = 2\left(1 - J_3 \frac{\Pi(z)}{z}\right)\frac{z^2}{J_1}, \tag{36}$$

which defines integral curves in the (z, s) space.

Using the constants of motion, we choose a set of dynamical variables as $\boldsymbol{\zeta} = (J_1, J_3, \rho_1, z)$. Then, the differential equation for (J_1, J_3, z) takes the simplest expression that $\partial_t J_1 = 0$, $\partial_t J_3 = 0$, and

$$\partial_t z = -z + J_3 \Pi(z). \tag{37}$$

Importantly, the time evolution of z is independent of ρ_1. Besides, the initial condition (26) leads to $J_1 = 4R$ and $J_2 = 1$; thus, $J_3 = 2R$. To sum up, the dynamical behavior of the edge deletion process of random graphs is described by

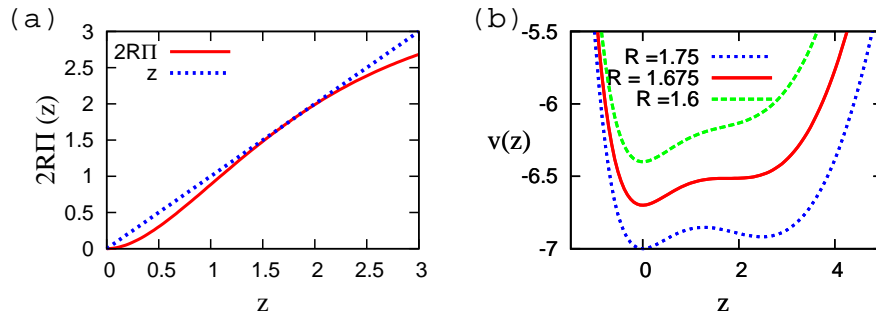$$\partial_t z = -z + 2R\Pi(z) \tag{38}$$

with $z(0) = 2R$.

Figure 3. (a) The graphs of z and $2R\Pi(z)$ with $R = 1.675$. Two intersection points appear when R is increased, while no intersection when R is decreased. (b) Shapes of potential functions $V(z)$ for the cases that $R \simeq R_{\rm c}$, $R < R_{\rm c}$ and $R > R_{\rm c}$, respectively.

The differential equation given in (38) can be easily analyzed. First, there exists the trivial solution $z = 0$. Then, let z_* be another fixed point (if it exists). $z_*(\neq 0)$ satisfies $z_* = 2R\Pi(z_*)$. From Fig. 3, we find that two nontrivial solutions exist when

$R > R_c$, where R_c is determined by $\min_{z>0}[z - 2R_c\Pi(z)] = 0$, which yields the compact expression of R_c as

$$R_c = \frac{1}{2}\min_{z>0}\left(\frac{z}{\Pi(z)}\right).$$ (39)

We numerically calculated $R_c \simeq 1.675$. In order to investigate the solution trajectory of (37), we express (37) in the form

$$\partial_t z = -\frac{dV}{dz},$$ (40)

where the potential function $V(z)$ is given by $V(z) = z^2/2 - 2R(z + 2e^{-z} + ze^{-z})$. We display the shape of the potential $V(z)$ in Fig. 3. It is seen that there are a pair of minimum and maximum in addition to the trivial minimum point $z = 0$ when $R > R_c$. Obviously, the solution corresponding to the maximum (saddle) is unstable, while the solution corresponding to the minimum (node) is stable. Note that the potential is a monotonic increasing function in z when $R < R_c$, which corresponds to the fact that there is no nontrivial stationary solution when $R < R_c$. The qualitative change of trajectories at $R = R_c$ is called a *saddle-node bifurcation*. The fixed point at $R = R_c$ is the *marginal saddle*, which is denoted by $z_c(= z_*(R_c))$. Since the condition $z(t \to \infty) \neq 0$ represents the existence of a k-core, R_c is the k-core percolation point. This determination method of R_c is essentially equivalent to that in Ref. [1]. The achievement of this study is the identification of the bifurcation type observed in the dynamics of k-core percolation in a random graph.

Now, we investigate the behavior of the system with $R = R_c - \epsilon$, where ϵ is a small positive constant. We define a dynamical variable ϕ by $z = z_c + \phi$. Substituting it into (38), we obtain

$$\partial_t \phi = -\epsilon a - b\phi^2 + O(\phi^3),$$ (41)

where $a = 2\Pi(z_c)$ and $b = -R_c\Pi''(z_c)$. Since the solution $\phi(t)$ is expressed as a scaling form

$$\phi(t) = \epsilon^{1/2}\Phi(\epsilon^{1/2}t),$$ (42)

the typical time for exiting the marginal saddle is proportional to $\epsilon^{-1/2}$.

5. Critical fluctuation

Next, we study the fluctuations that are described by the Langevin equation (25). Since the deterministic equation for $\boldsymbol{\zeta}$ is the simplest one, we rewrite the Langevin equation by using $\boldsymbol{\zeta}$. Formally, we express the variable transformation from $\boldsymbol{\rho}$ to $\boldsymbol{\zeta}$ as $\boldsymbol{\zeta} = \boldsymbol{\phi}(\boldsymbol{\rho})$. Then, using Ito's formula, one can derive

$$\partial_t z = -z + J_3\Pi(z) + \sum_{jl}\frac{\partial z}{\partial \rho_j}\sqrt{\frac{1}{n}}G_{jl}\xi_l + \frac{1}{n}\sum_{jl}\frac{\partial^2 z}{\partial \rho_j \partial \rho_l}A_{jl},$$ (43)

where the expression $\partial z/\partial \rho_j$ is evaluated from the functional dependence of z on $\boldsymbol{\rho}$. It should be noted that J_3 fluctuates in the Langevin description.

Concretely, we investigate the divergent behavior of the quantity

$$\chi_z(t) = n(\langle z(t)^2 \rangle - \langle z(t) \rangle^2) \tag{44}$$

for the system with $R = R_c - \epsilon$, where ϵ is a small positive constant. Here, it is naturally expected that the divergent part of the fluctuations of $h(t)$ is identical to that of $z(t)$. We therefore conjecture that $\chi_z(t)$ has a peak at $t = t_*$ and that t_* and $\chi_z(t_*)$ exhibit the power-law divergences $t_* \simeq \epsilon^{-\zeta}$ and $\chi_z(t_*) \simeq \epsilon^{-\gamma}$. We shall derive these divergences theoretically.

The perturbative calculation with respect to the nonlinearity in (43) seems quite difficult to capture the divergent behavior of $z(t)$. Instead, we utilize the bifurcation structure, as done in Ref. [14]. Following the idea of the method, we first notice two solutions of (38) with $R = R_c$. One solution z_u satisfies the conditions $z_u(t) \to z_c$ for $t \to -\infty$, $z_u(t) \to 0$ for $t \to \infty$, and $z_u(0) = z_0$, (say, $z_0 = 0.5$). The other solution $z_B(t)$ satisfies the conditions $z_B(t) \to z_c$ for $t \to \infty$ and $z_B(0) = z(0)$. $z_B(t)$ represents the down-hill trajectory to the marginal saddle from the point z_0 in the potential shape. Then, we express the trajectories by using the exit time θ from the marginal saddle as

$$z(t) = z_u(t - \theta) + (z_B(t) - z_c) + \varphi(t - \theta), \tag{45}$$

where $\varphi(t - \theta)$ represents a deviation from the superposition of the two solutions.

It is worthwhile to note that the variable θ corresponds to the Goldstone mode associated with the time-translational symmetry. Thus, the fluctuation of θ carries a divergent part, while φ can be treated as a variable slaved to θ. Based on this observation, $\langle z(t) \rangle$ and $\chi_z(t)$ can be estimated by the statistical average over θ. Note that we have devised a theoretical framework in which the statistical distribution of θ can be calculated perturbatively by considering the interaction of θ with $(z_B(t) - 1)$ [14, 15]. In the argument below, without entering this lengthy calculation, we shall determine phenomenologically the exponents characterizing the divergent behavior of $\chi_z(t)$.

We first calculate the exponents characterizing the divergences of $\langle \theta \rangle$ and the intensity of fluctuation χ_θ defined by

$$\chi_\theta \equiv n(\langle \theta^2 \rangle - \langle \theta \rangle^2). \tag{46}$$

We start with the scaling relations

$$\langle \theta \rangle = n^{\zeta'/\nu_*} f_1(n^{1/\nu_*} \epsilon), \tag{47}$$

$$\chi_\theta = n^{\gamma'/\nu_*} f_2(n^{1/\nu_*} \epsilon), \tag{48}$$

for large n and small ϵ, where we have introduced the exponents ζ', ν_*, and γ'. We here assume that $f_1(0) = \text{const}$ and $f_2(0) = \text{const}$. We also assume that $f_1(x) \simeq x^{-\zeta'}$ and $f_2(x) \simeq x^{-\gamma'}$ for $x \gg 1$, because $\langle \theta \rangle$ and χ_θ are expected to be independent of n in the regime $x \gg 1$. We find that $\zeta' = 1/2$ from (42). Furthermore, from (47), we assume that a distribution function of θ is expressed as an n-independent function of $\theta n^{-\zeta/\nu_*}$ when $\epsilon = 0$. This leads to a relation $\gamma'/\nu_* = 2\zeta'/\nu_* + 1$, which yields

$$\gamma' = 2\zeta' + \nu_*. \tag{49}$$

To this point, we have avoided the analysis of (43). In order to determine the value of ν_*, we need to study the equation. For the sake of a simple argument, we assume that the behavior near the saddle-node bifurcation point is described by (41) with a noise term:

$$\partial_t \phi = -\epsilon a - b\phi^2 + \sqrt{\frac{d}{n}}\eta, \tag{50}$$

where η satisfies $\langle \eta(t)\eta(t')\rangle = \delta(t - t')$, and d is a constant. Here, we have ignored effects of fluctuations of J_3 and the variable dependence of noise intensity. It is a non-trivial mathematical problem to clarify whether these simplifications are allowed in the description of critically divergent fluctuations. *

Once we are allowed to use (50), we can determine the value of the exponent ν_* as follows. We set $\epsilon = 0$ and write the weight for trajectories $[\phi] = (\phi(t))_{0 \leq t \leq \infty}$:

$$\mathcal{P}([\phi]) = \frac{1}{Z}\exp\left[-\frac{n}{2d}\int dt\{(\partial_t\phi + b\phi^2)^2 - \frac{d}{n}2b\phi\}\right], \tag{51}$$

where the last term originates from the Jacobian term associated with the transformation from η to ϕ. Now, we define a new scaled variable $\Phi(s)$ by $\phi(t) = n^{-1/3}\Phi(s)$ with a scaled time $s = n^{-1/3}t$. Substituting this into (51), we can confirm that the distribution function of trajectories $\Phi(s)$ is independent of n. This implies that the time scale near the marginal saddle is proportional to $n^{1/3}$. This yields $\zeta'/\nu_* = 1/3$. Recalling $\zeta' = 1/2$, we have arrived at $\nu_* = 3/2$. From (49), we also obtain $\gamma' = 5/2$. The result is summarized as follows.

$$\langle\theta\rangle = n^{1/3}f_1(n^{2/3}\epsilon), \tag{52}$$

$$\chi_\theta = n^{5/3}f_2(n^{2/3}\epsilon). \tag{53}$$

From these, $\langle\theta\rangle \simeq \epsilon^{-1/2}$ and $\chi_\theta \simeq \epsilon^{-5/2}$ in the regime $O(n^{-2/3}) \ll \epsilon \ll O(n^0)$. It should be noted that (52) and (53) have been confirmed numerically for a simple stochastic differential equation whose local form near the marginal saddle is equivalent to (50) [15].

Now, using this result, we calculate $\langle z(t)\rangle$ and $\chi_z(t)$ in the regime $O(n^{-2/3}) \ll \epsilon \ll O(n^0)$, where θ is expected to obey the Gaussian distribution

$$P(\theta) = \frac{1}{Z_\theta}e^{-n\frac{(\theta - \langle\theta\rangle)^2}{2\chi_\theta}} \tag{54}$$

with the normalization constant Z_θ. Defining the Fourier transform of $z_u(t)$ as

$$z_u(t) = \int \frac{d\omega}{2\pi}\tilde{z}_u(\omega)e^{i\omega t}, \tag{55}$$

we write approximate expressions

$$\langle z(t)\rangle \simeq \int \frac{d\omega}{2\pi}\tilde{z}_u(\omega)e^{i\omega t}\left\langle e^{-i\omega\theta}\right\rangle, \tag{56}$$

---

* Some trajectories satisfy $z(\infty) \geq z_c$, even when $R < R_c$. Such a behavior can be described by (43), but not by (50). Therefore, the argument below cannot be applied to the calculation of $\langle z(\infty)\rangle$, for example. Nevertheless, we expect that statistical properties of θ are described by (50) when we restrict the trajectories $z(\infty) \simeq 0$.

and

$$\langle z(t)^2 \rangle \simeq \int \frac{d\omega}{2\pi} \int \frac{d\omega'}{2\pi} \tilde{z}_{\mathrm{u}}(\omega) \tilde{z}_{\mathrm{u}}(\omega') \mathrm{e}^{i(\omega+\omega')t} \left\langle \mathrm{e}^{-i(\omega+\omega')\theta} \right\rangle. \tag{57}$$

The Gaussian distribution (54) immediately leads us to

$$\langle z(t) \rangle \simeq \int \frac{d\omega}{2\pi} \tilde{z}_{\mathrm{u}}(\omega) \mathrm{e}^{i\omega(t-\langle\theta\rangle)} \mathrm{e}^{-\frac{\chi_\theta \omega^2}{2n}}, \tag{58}$$

and

$$\langle z(t)^2 \rangle \simeq \int \frac{d\omega}{2\pi} \int \frac{d\omega'}{2\pi} \tilde{z}_{\mathrm{u}}(\omega) \tilde{z}_{\mathrm{u}}(\omega') \mathrm{e}^{i(\omega+\omega')(t-\langle\theta\rangle)} \mathrm{e}^{-\frac{\chi_\theta (\omega+\omega')^2}{2n}}. \tag{59}$$

Using these, we can derive

$$\chi_z(t) \simeq \chi_\theta \sum_{k=1}^{\infty} \left(\frac{1}{k!} \left(\sqrt{\frac{\chi_\theta}{n}} \right)^{k-1} \partial_t^k \langle z(t) \rangle \right)^2. \tag{60}$$

Here, let $\tau_{\mathrm{w}} = \sqrt{\chi_\theta/n}$ be the width of the distribution of θ. We expect that $\langle z(t) \rangle$ can be estimated as $z_{\mathrm{u}}(t - \langle\theta\rangle)$ in the regime $\tau_{\mathrm{w}} \ll 1$, where this regime is expressed as $O(n^{-2/5}) \ll \epsilon \ll O(n^0)$. Then, from (60), we obtain

$$\chi_z(t) \simeq \chi_\theta (\partial_t z_{\mathrm{u}}(t))^2, \tag{61}$$

from which we find that $\chi_z(t)$ takes a maximum at $t = t_*$, where $t_* \simeq \langle\theta\rangle \simeq \epsilon^{-1/2}$ and $\chi_z(t_*) \simeq \chi_\theta \simeq \epsilon^{-5/2}$. Since the fluctuation intensity is defined as the value of $\chi_z(t)$ in the limit $n \to \infty$ with small ϵ fixed, we conclude that $\zeta = 1/2$ and $\gamma = 5/2$. The behavior of $\chi(\tau)$ in the regime $O(n^{-2/3}) \ll \epsilon \ll O(n^{-2/5})$, which is described by (60), seems complicated. We conjecture that there is no power-law behavior in this regime.

6. Concluding remarks

We have demonstrated that the edge deletion processes of random graphs exhibit the saddle-node bifurcation in the deterministic limit, as shown in (41). The discontinuous transition of $\langle \bar{h}(t=\infty) \rangle$, from 0 to $Q(z_{\mathrm{c}})$, is understood from the nature of the bifurcation of trajectories of $z(t)$. (See (35) for the transformation from z to $\bar{h}$ in the deterministic description.) We can also understand the divergent behavior of $\chi(t)$ on the basis of critical fluctuations of exit time from the marginal saddle associated with the saddle-node bifurcation.

The numerical analysis of the power-law divergences is quite difficult, although the increasing trends of $\chi(\tau)$ and τ are easily observed, as already shown in Fig. 2. For example, consider the power-law divergence $\chi(\tau) \simeq \epsilon^{-5/2}$ in the regime $0.01 \le \epsilon \le 0.1$. In this case, we need to investigate the system with $n \gg 10^5$. However, since our computational algorithm does not involve any tactical steps, we cannot perform numerical experiments of such a large system.

Nevertheless, in Fig. 4, we present the numerical result of random graphs on $n = 2^{13}$ vertices. The square symbols represent τ and $\chi(\tau)$ for several values of ϵ. In order to complement the numerical data, we also display the results of numerical simulations of
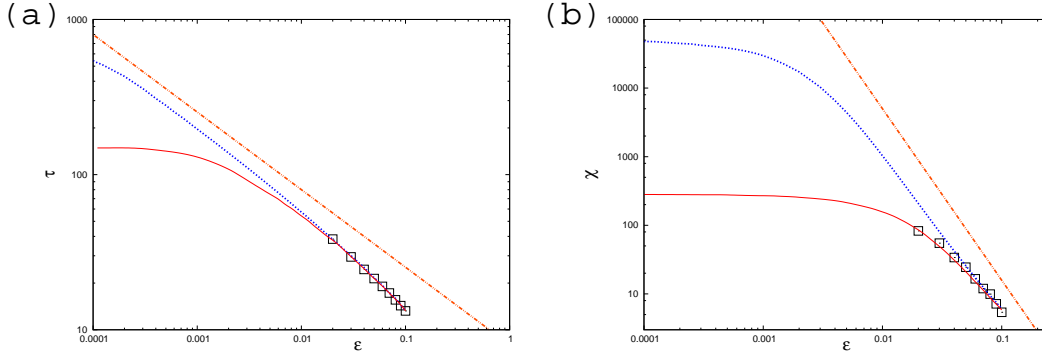
Figure 4. (a) τ as a function of ϵ. (b) $\chi(\tau)$ as a function of ϵ. The square symbols represent the numerical results of the k-core percolation dynamics with $n = 2^{13}$. The solid and dotted curves represent the numerical results of a Langevin equation with a small noise intensity that corresponds to the cases $n = 2^{13}$ and $n \simeq 2^{22}/3$, respectively, in the k-core percolation problem. The guide lines represent $\tau = 8\epsilon^{-0.5}$ and $\chi = 0.1\epsilon^{-2.5}$.

a simple Langevin equation whose local form near the marginal saddle is equivalent to (50). The equation is $\partial_t \phi = -\phi((\phi-1)^2 + \epsilon) + \sqrt{2T}\xi$, where $\langle \xi(t)\xi(t') \rangle = \delta(t-t')$ and T is the noise intensity which is expected to be proportional to $1/n$ in the present problem. The solid curve corresponds to the case $T = 2^{-11}/3$, whose value is chosen such that the square symbols are on the solid curves. Then, by decreasing the noise intensity to $T = 2^{-20}$, which might correspond to the k-core problem with $n \simeq 2^{22}/3$, we obtain the dotted curve. As discussed theoretically, the power-law behavior of $\chi \simeq \epsilon^{-5/2}$ is observed in the regime $O(n^{-2/5}) \ll \epsilon \ll O(n^0)$, and $\tau \simeq \epsilon^{-1/2}$ is observed in the regime $O(n^{-2/3}) \ll \epsilon \ll O(n^0)$.

With regard to finite size effects, we mention that the probability of finding trajectories satisfying $h(\infty) \neq 0$ is given by a universal function of $n^{1/2}(\epsilon - 2n^{-2/3})$.♯ This implies that the system behavior in the regime $\epsilon \leq O(n^{-1/2})$ is qualitatively different from that in the regime $\epsilon \geq O(n^{-1/2})$. Theoretically, in order to describe the crossover around $O(n^{-1/2})$, we need to analyze (43), not (50). When we are interested in the relaxation behavior, we should focus on the regime $\epsilon \geq O(n^{-1/2})$.

It is worthwhile to note that χ_θ exhibits the simpler behavior than $\chi(\tau)$. We therefore conjecture that χ_θ is a more fundamental quantity than $\chi(t)$. We also mention that the critical behavior of exit time from a marginal saddle is observed in a coupled oscillator model [17] related to neuronal avalanches [18]. (See also Ref. [19].) It is an interesting subject to find other examples belonging to the same universality class.

Although the k-core percolation is not directly related to jamming transitions, our results might provide a suggestion for future studies on jamming transition. As one example of such a study, we may theoretically consider the numerical result obtained for the jamming transition in the Frederic-Andersen model in a random graph [20],

♯ This result was confirmed numerically by the direct simulations of the dynamics we consider. See also Ref. [16] as a mathematical argument.

because the k-core percolation dynamics is regarded as an irreversible version of a kinetic constraint model. As another direction of study, one may analyze fluctuations of exit time in more general jamming systems. The important example is the application to the spherical p-spin glass model, for which the mode coupling theory is believed to be exact [21]. Since the transition described by this theory is interpreted as a variant of saddle-node bifurcation [22], we might discuss the divergent behavior of the so-called nonlinear susceptibility χ_4 on the basis of the exit time from the plateau regime.

Finally, we consider the k-core percolation in finite dimensional systems. In general, one may conjecture that a transition is smeared in a manner similar to bootstrap percolation problems [23]. (See Refs. [24] and [25] for attempts of studying the k-core percolation in finite dimensional systems.) From our viewpoint, as the first stage of a study on finite dimensional systems, we should identify the upper-critical dimension d_c for a diffusively coupled model of a simple stochastic system undergoing a saddle-node bifurcation. With regard to this problem, we point out that ν_* might be related to the exponent ν that characterizes the divergence of the length scale as $\nu = \nu_*/d_c$ [26]. Furthermore, in the next stage of studying finite dimensional systems, we should consider an equivalence or inequivalence between such a coupled model and the k-core percolation dynamics in a finite dimensional lattice. The analysis developed in the present study may be useful in this consideration.

Acknowledgments

References

[1] Pittel B, Spencer J, and Wormald N 1996 J. Combin. Theory B **67** 111
[2] Chalupa J, Leath P L, and Reich G R 1979 J. Phys. C: Solid State Phys. **12** L31
[3] Monkarzel C, Duxbury P M, Leath P L 1997 Phys. Rev. E **55** 5800
[4] Schwartz J M, Liu A J, and Chayes L Q 2006 Europhys. Lett. **73** 560
[5] Silbert L E, Liu A J, and Nagel S R 2005 Phys. Rev. Lett. **95** 098301
[6] Dorogovtsev S N, Goltsev A V, 2006 and Menders J F F Phys. Rev. Lett. **96** 040601
[7] Goltsev A V, Dorogovtsev S N, and Menders J F F 2006 Phys. Rev. E **73** 056101
[8] Farrow C L, Duxbury P M and Moukarzel C 2005 Phys. Rev. E **72** 066109
[9] Sabhapandit S, Dhar D and Shukla P 2002 Phys. Rev. Lett. **88**, 197202
[10] Farrow C L, Shukla P and Duxbury P M 2007 J. Phys. A: Math. Theor. **40** F581
[11] Biroli G and Bouchaud J P 2004 Europhys. Lett. **67** 21
[12] Toninelli C, Biroli G, and Fisher D S 2006 Phys. Rev. Lett., **96**, 035702
[13] Biroli G, Bouchaud J P, Miyazaki K, and Reichman D R 2006 Phys. Rev. Lett. **97** 195701

[14] Iwata M and Sasa S 2007 Europhys. Lett. **77**, 50008
[15] Iwata M and Sasa S 2008 in preparation
[16] Dembo A and Montanari A, 2008 arXiv:math/0702007, to appear in Ann. Appl. Prob.
[17] Ohta H and Sasa S 2008 arXiv:0805.4671
[18] Plentz D and Thiagarajan T C 2007 Trends in Neurosci. **30** 101
[19] Lindner B, Longtin A, and Bulsara A 2003 Neural Comp. **15** 1761
[20] Sellitto M, Biroli G and Toninelli C 2005 Europhys. Lett. **69** 496
[21] Crisanti A, Horner H, Sommers H J 1993 Z. Phys. B **92** 257
[22] Iwata M and Sasa S 2008 in preparation
[23] Aizenman M and Lebowitz J L 1988 J. Phys. A: Math. Gen. **21** 3801
[24] Harris A B and Schwartz J M 2005 Phys. Rev. E **72** 046123
[25] Parisi G and Rizzo T 2006 arXiv:cond-mat/0609777, to appear in Phys. Rev. E (2008)
[26] Botet R, Jullien R, and Pfeuty P 1982 Phys. Rev. Lett. **49** 478